

# Ab initio study of canted magnetism of finite atomic chains at surfaces

B. Lazarovits<sup>†</sup>, B. Újfalussy<sup>‡</sup>, L. Szunyogh<sup>†§†</sup>, G. M. Stocks<sup>‡</sup> and P. Weinberger<sup>†</sup>

<sup>†</sup> Center for Computational Materials Science, Technical University Vienna, A-1060, Gumpendorferstr. 1.a., Vienna, Austria

<sup>‡</sup> Metals and Ceramics Division, Oak Ridge National Laboratory, Oak Ridge, Tennessee 37831, USA

<sup>§</sup> Department of Theoretical Physics and Center for Applied Mathematics and Computational Physics, Budapest University of Technology and Economics, Budafoki út 8, H-1111, Budapest, Hungary

**Abstract.** By using ab initio methods on different levels we study the magnetic ground state of (finite) atomic wires deposited on metallic surfaces. A phenomenological model based on symmetry arguments suggests that the magnetization of a ferromagnetic wire is aligned either normal to the wire and, generally, tilted with respect to the surface normal or parallel to the wire. From a first principles point of view, this simple model can be best related to the so-called magnetic force theorem calculations being often used to explore magnetic anisotropy energies of bulk and surface systems. The second theoretical approach we use to search for the canted magnetic ground state is first principles adiabatic spin dynamics extended to the case of fully relativistic electron scattering. First, for the case of two adjacent Fe atoms on a Cu(111) surface we demonstrate that the reduction of the surface symmetry can indeed lead to canted magnetism. The anisotropy constants and consequently the ground state magnetization direction are very sensitive to the position of the dimer with respect to the surface. We also performed calculations for a seven-atom Co chain placed along a step edge of a Pt(111) surface. As far as the ground state spin orientation is concerned we obtain excellent agreement with experiment. Moreover, the magnetic ground state turns out to be slightly noncollinear.

PACS numbers: 75.10.Lp, 75.30.Gw, 75.75.+a

## 1. Introduction

Magnetic devices on the atomic scale became recently a subject of intensive experimental and theoretical research (see, e.g., the "viewpoint" drawn by Kübler [1]). Understanding and design of the relevant physical properties – magnetic moments, magnetic anisotropy energies, thermal stability, switching – of atomic scaled magnets demand a detailed knowledge of their electronic and magnetic structure. For this reason a considerable amount of theoretical work has been published to investigate the – mostly noncollinear – magnetic ground state of free and supported metallic clusters [2, 3, 4, 5, 6, 7, 8].

<sup>†</sup> To whom correspondence should be addressed. E-mail: szunyogh@heisenberg.phy.bme.hu

Quite recently, Gambardella *et al.* reported well characterized experiments on linear chains of about 80 Co atoms located at a step edge of a Pt(111) surface terrace [9]. At 45 K the formation of ferromagnetic spin-blocks of about 15 atoms was found with an easy magnetization axis normal to the chain and pointing along a direction of  $43^\circ$  towards the step edge. Stimulated mainly by this experiment, in the present work we present a study of the magnetic ground state of linear atomic chains deposited on a fcc(111) host surface. We first focus on the origin of the unusual canted magnetism. In the case of two adjacent Fe atoms placed into a Cu(111) surface we investigate how the orientation of the magnetization depends on the position of the dimer with respect to the surface. Then we calculate and analyze in some detail the ground state spin configuration of a finite Co chain at a Pt(111) step edge.

## 2. Theoretical methods

Let us write the magnetic moment of a ferromagnetic system in terms of spherical coordinates,  $\mathbf{M} = M(\sin \theta \cos \phi, \sin \theta \sin \phi, \cos \theta)$ , where  $0 \leq \theta \leq \pi$  and  $0 \leq \phi \leq 2\pi$  are the azimuthal and polar angles in a usual rectangular reference of frame, and assume that the magnitude of the magnetic moment,  $M$ , is independent on the the orientation. In case of a linear chain of atoms deposited along the  $x$  axis of an fcc(111) lattice (see, e.g., figure 1) the system has at best one symmetry operation, namely, a mirror symmetry with respect to the  $(y, z)$  plane, therefore, invariance of the energy implies up to second order in the magnetization that

$$E(\theta, \phi) = E_0 + K_{2,1} \cos 2\theta + K_{2,2}(1 - \cos 2\theta) \cos 2\phi + K_{2,3} \sin 2\theta \sin \phi, \quad (1)$$

where  $K_{2,i}$  ( $i = 1, 2, 3$ ) are so-called anisotropy constants. Solving the corresponding Euler-Lagrange equations results that, depending on the actual values of the anisotropy constants, the easy magnetization axis corresponds either to  $\phi = \pi/2$  and  $\theta \in \{\theta_0, \theta_0 + \pi/2, \theta_0 + \pi\}$ , where

$$\theta_0 = \frac{1}{2} \arctan \left( \frac{K_{2,3}}{K_{2,1} + K_{2,2}} \right) \quad \left( -\frac{\pi}{4} < \theta_0 < \frac{\pi}{4} \right), \quad (2)$$

or to  $\theta = \pi/2$  and  $\phi = 0$ . Clearly, only in the special case of  $K_{2,3} = 0$  can the ground state magnetization point along the  $z$  axis (perpendicular to the planes).

The so-called magnetic force theorem (MFT) represents a straightforward and relatively simple way to calculate anisotropy constants as based on the local spin density approximation (LSDA). Here, a self-consistent calculation is carried out for only one selected orientation of the magnetization. Then, by keeping these potentials and effective fields fixed, the orientation of the spin-magnetization (in LSDA parallel to the effective field) is varied, whereby – neglecting further self-consistency – only the single-site (band) energy is considered, see reference [10] for several applications of this method in ordered and disordered layered systems. Note that, in principle, also the magnetic dipole-dipole interaction energy has to be added to the bandenergy. For the case of small nanostructures the estimated magnitude of this energy is, however, by at least one order less than that of the bandenergy.

A numerically efficient tool to search for an equilibrium spin arrangement is to trace the time evolution of the spin moments until a stationary state is achieved. According to the so-called first principles adiabatic spin-dynamics (SD) founded by Antropov *et al.* [11], for a system with well-defined local (atomic) moments the

evolution of the time dependent orientational configuration,  $\{\mathbf{e}_i(t)\}$ , is described by a microscopic, quasi-classical equation of motion,

$$\frac{d\mathbf{e}_i}{dt} = \gamma \mathbf{e}_i \times \mathbf{B}_i^{eff} + \lambda \left[ \mathbf{e}_i \times (\mathbf{e}_i \times \mathbf{B}_i^{eff}) \right], \quad (3)$$

where  $\mathbf{B}_i^{eff}$  is an effective magnetic field averaged over cell  $i$ ,  $\gamma$  is the gyromagnetic ratio and  $\lambda$  is a damping (Gilbert) parameter. Following the arguments of Stocks *et al.* [12, 13] in this equation at any moment of time the orientational state has to be evaluated within a constrained density functional theory (DFT). Here a local constraining field,  $\mathbf{B}_i^{con}$  ensures the stability of a non-equilibrium orientational state. This implies that the internal effective field that rotates the spins in the absence of a constraint and, therefore, has to be used in equation (3) is just the opposite of the constraining field [12]. By merging with the locally selfconsistent multiple scattering (LSMS) method SD has been applied so far to bulk metals and alloys [12, 13, 14] and, very recently, to interfaces [15].

In order to deal with exchange splitting and relativistic scattering on equal theoretical footing we combined the first principles SD scheme based on constrained DFT by solving the Kohn–Sham–Dirac equation,

$$[c\boldsymbol{\alpha} \cdot \mathbf{p} + \beta mc^2 + V(\mathbf{r}) + \mu_B \beta \boldsymbol{\sigma} \cdot (\mathbf{B}^{xc}(\mathbf{r}) + \mathbf{B}^{con}(\mathbf{r})) - E] \psi(\mathbf{r}) = 0, \quad (4)$$

where  $\boldsymbol{\alpha}$  and  $\beta$  are the usual Dirac matrices,  $\boldsymbol{\sigma}$  are the Pauli matrices,  $V(\mathbf{r})$  stands for the Hartree and the exchange–correlation potential, while within the local spin density approximation (LSDA)  $\mathbf{B}^{xc}(\mathbf{r})$  is an exchange field interacting only with the spin of the electron. Equations (3) and (4) form the very basis of a relativistic *spin-only* dynamics, inasmuch no attempt is made to explicitly trace the time evolution of the orbital moments.

In conjunction with both the MFT and the SD we applied the multiple scattering Green’s function embedded cluster method developed by Lazarovits *et al.* [16]. In here, first a self-consistent calculation is carried out for the surface system in terms of the relativistic Screened Korringa–Kohn–Rostoker (SKKR) method [17], and then the nanostructure is embedded into this host according to the equation

$$\boldsymbol{\tau}^r(\epsilon) = \boldsymbol{\tau}^r(\epsilon) \left[ \mathbf{I} - (\mathbf{t}^r(\epsilon)^{-1} - \mathbf{t}^c(\epsilon)^{-1}) \boldsymbol{\tau}^c(\epsilon) \right]^{-1}, \quad (5)$$

where  $\boldsymbol{\tau}^r(\mathbf{t}^r)$  and  $\boldsymbol{\tau}^c(\mathbf{t}^c)$  are site–angular momentum matrices of the scattering path operators (single–site  $t$  operators) of the host surface system and the cluster, respectively, and  $\epsilon$  is the energy. By solving also the corresponding Poisson equation with appropriate boundary conditions a selfconsistent calculation for the selected cluster can be performed that takes full account of the environment [16]. It is important to underline that this description does not rely on periodic boundary conditions applied to the (embedded) cluster. In all calculations we used the atomic sphere approximation (ASA) and an angular momentum expansion up to  $\ell_{max} = 2$ .

### 3. Two Fe impurities at Cu(111) surfaces

The simplest system that reduces the symmetry of the fcc(111) layers to only one mirror plane is a pair of nearest neighbour defects as illustrated in figure 1. We embedded two such Fe impurities on top, i.e., into the first vacuum layer (labelled by  $S + 1$ ), into the surface ( $S$ ) layer and into the subsurface ( $S - 1$ ) layer of a Cu(111) surface. First a self-consistent SKKR calculation has been performed by relaxing the

potentials of 6 Cu layers and 3 empty sphere layers in order to describe the surface region from the bulk to the vacuum. Then, by employing equation (5), for the three above cases the Fe dimers were calculated self-consistently. Since these calculations are intended provide only with qualitative predictions, for simplicity, we neglected relaxations of the potentials of the host atoms,

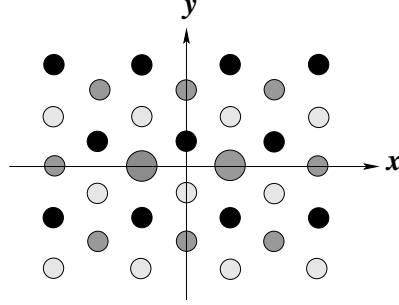


**Figure 1.** Schematic top view of two impurities (big shaded circles) placed into fcc(111) layers as nearest neighbours. The host atoms in the same layer are displayed by small shaded circles, those in the layer above by full circles, while those in the layer below by empty circles.

As mentioned before, the present implementation of our SD scheme serves (only) for finding the magnetic ground state of the system, therefore, it is sufficient to consider only the second (damping) term on the right hand side of equation (3). The evolution of the spin orientation is then measured on a time scale with a unit (time step) of  $1/\lambda$ . In figure 2 the evolution of the  $\theta$  and  $\phi$  angles and the magnitude of the constraining field are plotted in this artificial time scale for one of the Fe atoms. Note that during the SD procedure, the magnetic configuration of the two Fe atoms was confined to be symmetric with respect to the  $(y, z)$  plane. (We checked, however, that the final result is independent on the starting configuration.)

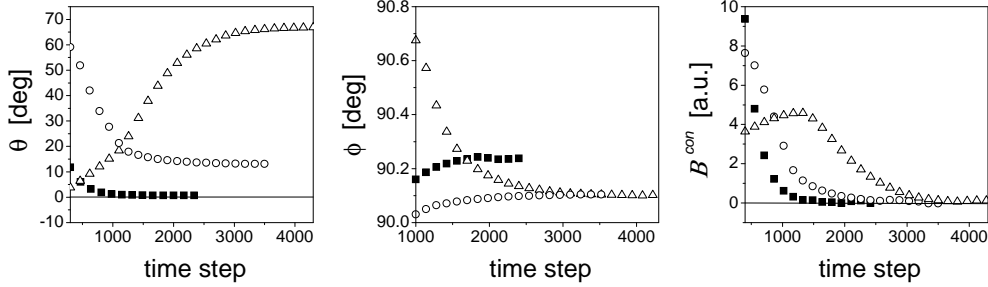


**Figure 2.** Evolution of the direction of magnetization and the magnitude of the constraining field according to a spin-dynamics calculation for two Fe impurities placed into different layers of a Cu(111) surface:  $\blacksquare$   $S + 1$ ,  $\triangle$   $S$ ,  $\circ$   $S - 1$ . For better visibility, the corresponding results for the first 300–1000 iterations are not shown. Displayed are only the data for one of the Fe atoms (see text).

Actually in a few time steps, for all the three layer positions the magnetic state of the two Fe atoms became nearly ferromagnetic and perpendicular to the line connecting the two impurities ( $\phi \simeq 90^\circ$ ). A satisfactory convergence was, however,

achieved only after thousands of time steps later, when – as can be seen from figure 2 – the constraining fields converged to zero. The final magnetic states can be summarized as follows:  $\theta = 0.73^\circ, 66.8^\circ$  and  $13.1^\circ$ , as well as  $\phi = 89.8^\circ, 89.9^\circ$  and  $89.9^\circ$  for one of the Fe atoms in layers  $S+1$ ,  $S$  and  $S-1$ , respectively, and a symmetric orientation for the other Fe atom. Clearly, these magnetic ground states are in qualitative agreement with the predictions of the simple phenomenological theory, see equations (1) and (2).

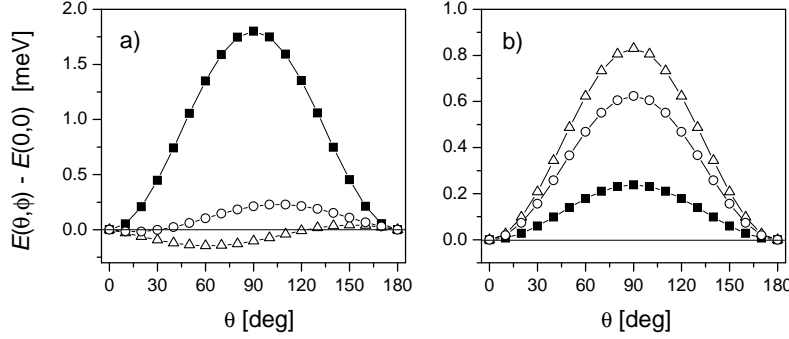


**Figure 3.** Bandenergy differences from MFT calculations for two Fe impurities at a Cu(111) surface:  $\blacksquare$   $S+1$ ,  $\triangle$   $S$ ,  $\circ$   $S-1$ ; a)  $\phi = 90^\circ$ , b)  $\phi = 0$ . Solid lines show curves fitted to equation 1 with the parameters contained by table 1.

**Table 1.** Anisotropy parameters (in units of meV), see equation (1), fitted to energies calculated within the MFT for two Fe impurities placed at different layers of a Cu(111) surface. The azimuthal angle corresponding to the global minimum of the energy is also displayed.

| layer<br>positions | $K_{2,1}$ | $K_{2,2}$ | $K_{2,3}$ | $\theta_0$    |
|--------------------|-----------|-----------|-----------|---------------|
| $S+1$              | -0.51     | -0.39     | -0.0026   | $0.083^\circ$ |
| $S$                | -0.18     | 0.23      | -0.079    | $62.0^\circ$  |
| $S-1$              | -0.21     | 0.10      | -0.065    | $15.7^\circ$  |

We carried out MFT calculations by using the output of the SD calculations. Figure 3 shows (band)energy curves when scanning the (uniform) direction of the magnetization through the paths  $0 < \theta < 180^\circ$  for  $\phi = 90^\circ$ , i.e., in the  $(y, z)$  plane and for  $\phi = 0^\circ$ , i.e., in the  $(x, z)$  plane. All the calculated data fit almost precisely the function in equation (1) with the parameters listed in table 1. For all the three cases the minimum of the energy is found in the  $(y, z)$  (symmetry) plane at an azimuthal angle,  $\theta$ , also shown in table 1. These angles coincide remarkably well with those obtained from the SD calculations. It should be noticed, however, that by using the output of self-consistent calculations with a magnetization fixed along the  $z$  axis, in particular, for an Fe dimer placed into layer  $S$  we obtained an apparently different ground state orientation ( $\theta = 46.5^\circ$ ). This clearly demonstrates that the applicability of MFT is quite limited.

It is obvious that a pair of Fe atoms in layer  $S+1$  represents the case of strong perpendicular anisotropy with a corresponding anisotropy energy of about 0.9 meV/Fe atom. This clearly explains the relatively fast convergence of the SD scheme, while in the other two cases due to the smaller spin-orbit coupling the convergence was much slower (see figure 2). For Fe dimers immersed into layers  $S$  and  $S-1$  a change

of the orientation from the  $z$  to the  $x$  direction costs much larger energy than a corresponding variation within the symmetry plane, because the otherwise remarkably reduced anisotropy constants,  $K_{2,1}$  and  $K_{2,2}$ , differ in sign. Concomitantly, the relative increase of the magnitude of  $K_{2,3}$  gives rise to a canted ground state, see equation (2). It should be noted that, similar to as discussed in Ref. [18], the change of the anisotropy constants,  $K_{2,i}$  with respect to the position of the Fe dimer can be related to the different hybridization between the electronic states of the Fe and the Cu atoms.

#### 4. Finite Co wire at the step edge of a Pt(111) surface

We first performed a calculation treating 8 layers of Pt selfconsistently together with 4 layers of vacuum. Then, a seven-atom chain of Co together with 10 empty (vacuum) spheres were embedded into the topmost Pt layer as schematically indicated in figure 4. Simultaneously all the nearest neighbours of the Co atoms were re-embedded into the respective Pt or vacuum layers to allow for the relaxation of potentials around the Co chain. Therefore, an embedded cluster of a total of 55 atoms was treated selfconsistently.

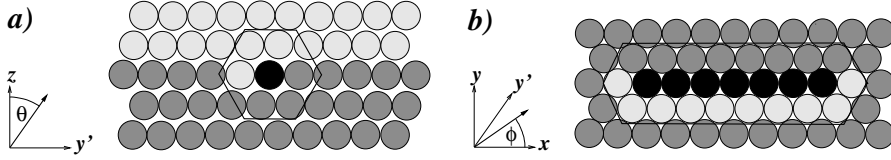


**Figure 4.** Schematic view of the geometry of a seven-atom Co chain along a Pt(111) step edge. Full circles: Co atoms, shaded circles: Pt atoms, open circles: empty spheres. **a)**: side view, **b)**: top view of the surface Pt layer with the Co chain. The cluster embedded is indicated by solid lines. The coordinate system gives reference to the azimuthal and polar angles,  $\theta$  and  $\phi$ , that characterize the orientation of the magnetization. (Note that in Ref. [9] a different coordinate system and the opposite notation for the angles is used.)

For each Co atom in the chain, in figure 5 the evolution of the  $\theta$  and  $\phi$  angles is plotted for the first 100 time steps in the artificial time scale mentioned in section 3. Initially the directions of the atomic magnetic moments were set by a random number generator. It can be seen that after some oscillations both the  $\theta$  and the  $\phi$  angles for all the Co atoms quickly approach to nearly the same value for all the Co atoms, i.e., as in the previous case of Fe dimers at a Cu(111) surface, to a nearly ferromagnetic configuration. The initial rapid oscillations that can be observed in figure 5 are the consequence of the relatively large constraining fields caused by large exchange energies whenever the moments point into very different directions. In about 1000 time steps the  $\phi$  angles, converged to  $90^\circ$ , with a spread of less than  $1^\circ$ , i.e., normal to the chain and the  $\theta$  angles converged to nearly  $42^\circ$ . All these results are in excellent agreement with experiment [9].

We also performed MFT calculations with the selfconsistent potentials and fields obtained from the SD procedure. The fitted anisotropy parameters  $K_{2,1} = -0.16$  meV,  $K_{2,2} = -1.06$  meV, and  $K_{2,3} = -4.81$  meV not only fairly well reproduce the easy axis,  $\theta = 38^\circ$  and  $\phi = 0^\circ$ , but also result in a value of the anisotropy energy (defined as the energy difference between the hard and the easy axes) of 1.42 meV/Co atom that satisfactorily compares with that derived from experiment (2.0 meV) [9].

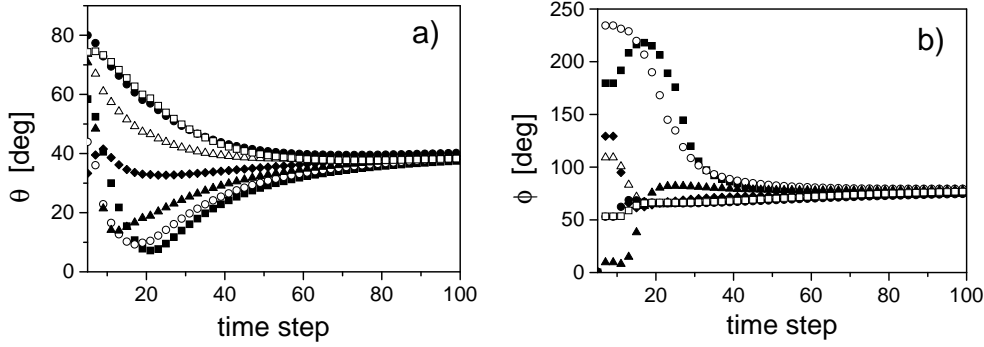


**Figure 5.** Evolution of the angles  $\theta$ , part a), and  $\phi$ , part b), defining the orientation of the spin moments for the seven Co atoms in the finite chain depicted in figure 4. The symbols refer to the following Co atoms numbered from the left to the right in part b) of figure 4:  $\blacksquare$  1,  $\circ$  2,  $\blacktriangle$  3,  $\blacklozenge$  4,  $\triangle$  5,  $\bullet$  6,  $\square$  7. Shown are only the first 100 time steps.

**Table 2.** Calculated magnitudes and orientations of the spin and orbital moments in a seven-atom Co chain along a Pt(111) step edge.

| atom | Spin moment       |                      | Orbital moment    |                      |
|------|-------------------|----------------------|-------------------|----------------------|
|      | moment( $\mu_B$ ) | $\Theta(\text{deg})$ | moment( $\mu_B$ ) | $\Theta(\text{deg})$ |
| 1    | 2.23              | 41.1                 | 0.25              | 39.1                 |
| 2    | 2.18              | 42.5                 | 0.20              | 41.5                 |
| 3    | 2.18              | 42.3                 | 0.19              | 40.1                 |
| 4    | 2.18              | 42.4                 | 0.20              | 41.3                 |
| 5    | 2.18              | 42.3                 | 0.19              | 40.2                 |
| 6    | 2.18              | 42.5                 | 0.20              | 41.5                 |
| 7    | 2.23              | 41.1                 | 0.25              | 39.1                 |

Extracted from the final (equilibrium) state, the size and the azimuthal angle  $\theta$  of the spin and orbital moments for each Co atom are shown in table 2. While the calculated spin moments for the inner Co atoms ( $2.18 \mu_B$ ) are in good agreement with the value deduced from experiment ( $2.12 \mu_B$ ) [9] and also with other theoretical studies on infinite wires [19, 20], the edge of the wire is characterized by larger spin (and orbital) moments [21]. Although our calculated orbital moments for the inner atoms ( $0.19\text{--}0.20 \mu_B$ ) are larger than the corresponding values from other LSDA calculations ( $0.16 \mu_B$  [19] and  $0.15 \mu_B$  [20]), they are still much too small when compared to the experimental value ( $0.68 \mu_B$ ) [9]. Note that including orbital polarization scheme or using the LDA+U method a value of  $0.92 \mu_B$  [19] and  $0.45 \mu_B$  [20] can be obtained.

As can be inferred from table 2 the spin moments of the inner atoms are fairly parallel, those at the end of the chain however, are off by more than  $1^\circ$ . This can be associated with the anisotropy energy contributions being larger at end of the chains than inside as found for finite Co wires deposited on a Pt(111) surface [21]. It can also be seen in table 2 that the orbital moments oscillate stronger in magnitude and orientation than the spin moments. As pointed out by Jansen [22], within the DFT the spin and orbital moments are required to align only when the ground state refers to a high-symmetry direction. This is, however, not the case for the Co wire since the ground state orientation is not directly induced by symmetry.

## 5. Summary

In this work we presented calculations of the magnetic ground state of linear atomic chains placed onto surfaces in terms of the magnetic force theorem and an ab-initio spin dynamics scheme. We found that due to the variation of the anisotropy constants the canted magnetic state obtained for a Fe dimer at a Cu(111) sensitively depends on its position. In excellent quantitative agreement with experiment, we obtained a canted ground state for a finite Co wire along a Pt(111) surface step edge. We also found that this magnetic state is noncollinear: a feature that is expected to play a key role in nanostructures of more complex geometry.

## Acknowledgments

Financial support was provided by the Center for Computational Materials Science (Contract No. GZ 45.531), the Austrian Science Foundation (Contract No. W004), the Research and Technological Cooperation Project between Austria and Hungary (Contract No. A-3/03) and the Hungarian National Scientific Research Foundation (OTKA T046267 and OTKA T037856). The work of BU and GMS was supported by DOE-OS, BES-DMSE under contract number DE-AC05-00OR22725 with UT-Battelle LLC. Calculations were performed at ORNL-CCS (supported by OASCR-MICS) and NERSC (supported by BES-DMSE).

## References

- [1] Kübler J 2003 *J. Phys.: Condens. Matter* **15** V21
- [2] Ojeda-López M A, Dorantes-Dávila J and Pastor G M 1997 *J. Appl. Phys.* **81** 4170
- [3] Oda T, Pasquarello A and Car R 1998 *Phys. Rev. Lett.* **80** 3622
- [4] Ivanov O and Antropov V P 1999 *J. Appl. Phys.* **85** 4821
- [5] Hobbs D, Kresse G and Hafner J 2000 *Phys. Rev. B* **62** 11556
- [6] Uzdin S, Uzdin V and Demangeat C 2001 *Comp. Mat. Sci.* **17** 441
- [7] Fujima N 2001 *Eur. Phys. J. D* **16** 185
- [8] Anton J, Fricke B and Engel E 2004 *Phys. Rev. A* **69** 012505
- [9] Gambardella P, Dallmeyer A, Maiti K, Malagoli M C, Eberhardt W, Kern K and Carbone C 2002 *Nature* **416** 301; Gambardella P 2003 *J. Phys.: Condens. Matter* **15** S2533
- [10] Weinberger P and Szunyogh L 2000 *Comp. Mat. Sci.* **17** 414
- [11] Antropov V P, Katsnelson M I, Harmon B N, van Schilfgaarde M and Kusnezov D 1996 *Phys. Rev. B* **54** 1019
- [12] Stocks G M, Újfalussy B, Xindong Wang, Nicholson D M C, Shelton W A, Yang Wang, Canning A and Györfy B L 1998 *Philos. Mag. B* **78** 665
- [13] Újfalussy B, Xindong Wang, Nicholson D M C, Shelton W A, Stocks G M, Yang Wang and Györfy B L 1999 *J. Appl. Phys.* **85** 4824
- [14] Stocks G M, Shelton W A, Schulthess T C, Újfalussy B, Butler W H and Canning A 2002 *J. Appl. Phys.* **91** 7355
- [15] Újfalussy B, Schulthess T C and Stocks G M 2003 *Computer Simulation Studies in Condensed-Matter Physics XV* (Eds. Landau D P, Lewis S P, Schüttler H B, Springer Proceedings in Physics) vol 90
- [16] Lazarovits B, Szunyogh L and Weinberger P 2002 *Phys. Rev. B* **65** 104441
- [17] Szunyogh L, Újfalussy B and Weinberger P 1995 *Phys. Rev. B* **51** 9552
- [18] Lazarovits B, Szunyogh L, Weinberger P and Újfalussy B 2003 *Phys. Rev. B* **68** 024433
- [19] Komelj M, Ederer C, Davenport J W and Fahnle M 2002 *Phys. Rev. B* **66** 140407
- [20] Shick A B, Máca F and Oppeneer P M 2003 *Preprint* arXiv:cond-mat/0312467
- [21] Lazarovits B, Szunyogh L and Weinberger P 2003 *Phys. Rev. B* **67** 024415
- [22] Jansen H J 1999 *Phys. Rev. B* **59** 4699